

A complete active space valence bond (CASVB) method

Kimihiko Hirao,^{a)} Haruyuki Nakano, and Kenichi Nakayama

Department of Applied Chemistry, Graduate School of Engineering, The University of Tokyo, Tokyo, Japan 113

Michel Dupuis

Environmental Molecular Sciences Laboratory, Pacific Northwest National Laboratory, Richland, Washington

(Received 8 July 1996; accepted 22 August 1996)

A complete active space valence bond (CASVB) method is proposed which is particularly adapted to chemical interpretation. A CASVB wave function can be obtained simply by transforming a canonical CASSCF function and readily interpreted in terms of the well known classical VB resonance structures. The method is applied to the ground and excited states of benzene, butadiene, and the ground state of methane. The CASVB affords a clear view of the wave functions for the various states. The electronic excitation is represented in a VB picture as rearrangements of the spin couplings or as charge transfers which involve breaking covalent bonds and forming new ionic bonds. The former gives rise to covalent excited states and the latter to ionic excited states. The physical reasons why it is so difficult to describe the ionic excited states at the CASSCF level with a single active space and why the lowest $1^1B_2^+$ state in *cis*-butadiene is so stabilized compared to the corresponding $1^1B_u^+$ state in the *trans* isomer are easily identified in view of a VB picture. The CASVB forms a useful bridge from molecular orbital theory to the familiar concepts of chemists.

© 1996 American Institute of Physics. [S0021-9606(96)01744-8]

I. INTRODUCTION

Recently, accurate *ab initio* quantum computational chemistry has evolved dramatically. The size of molecular systems, which can be studied accurately using *ab initio* methods is increasing very rapidly. Especially, multireference based perturbation theory, such as CASPT2 by Roos *et al.*¹ and our MRMP (multireference Møller–Plesset theory),² has opened a world of new possibilities. It can treat *real* systems with *predictive* accuracy. Computational quantum chemistry is becoming an integral part of chemistry research. Theory can now make very significant contributions to chemistry.

The Hartree–Fock (HF) model has a conceptual simplicity based on the intuitive idea that individual electrons move independently in the average field of all other electrons. We can now easily go beyond the HF approximation by making use of the highly sophisticated methods such as variational CI, perturbational, and cluster expansion methods. However, in the quest for accuracy, we lose the simplicity of the HF picture. It is rather complicated to analyze correlated wave functions. It is probably for this reason that too often quantum chemists nowadays discard the wave function and merely report that their computations have reproduced the molecular structures, heats of formation, vibrational energies, dipole moments, etc. The main interpretative information, however, is included in the wave function. The aim of accurate computations lies not in lowering the energy of the system, but in understanding physical and chemical laws hidden behind the phenomena from the first principle of quan-

tum mechanics. The interpretation of wave functions is the driving force of the present work.

Classical valence bond (VB) theory is very successful in providing a qualitative explanation for many aspects. Chemists are familiar with the localized molecular orbitals (LMO) and the classical VB resonance concepts. If modern accurate wave functions can be represented in terms of such well known concepts, chemists' intuition and experiences will give a firm theoretical basis and the role of the computational chemistry will undoubtedly expand.

In general, wave functions are invariant against linear transformations among the basis orbitals. The invariance affords a chemical interpretation of the molecular electronic distribution. Such a transformation may also contribute a useful bridge from the molecular orbitals (MO) to the familiar concepts of empirical chemistry and provide some insight into the nature of the electronic structure. In this paper, we will propose a CAS valence bond (CASVB) method which makes use of these invariant properties of the wave function.

The CASSCF³ or FORS (full optimized reaction space)⁴ method is an attempt to generalize the HF model to situations where the state-specific nondynamical correlation is important, while keeping the conceptual simplicity of the HF model as much as possible. It often generates far too many configurations but there are many advantages. Once the active space is chosen, the wave function is completely specified. It is size consistent and the wave function is invariant to the transformations among active orbitals. Although it does not include the transferable dynamical correlation, it provides a good starting point for such studies.

The CASVB functions can be obtained by transforming the canonical CASSCF functions without loss of energy. First we transform the CASSCF delocalized MO to localized

^{a)}Author to whom correspondence should be addressed.

MO using the arbitrariness in the definition of the active orbitals. Then we perform a full CI again in the active space. Here, we also use the arbitrariness in the definition of the expansion configuration functions. The configuration functions used are the bonded functions based on the LMOs with the Rumer spin eigenfunctions. This form of spin eigenfunctions plays a special role in the VB method. The CASVB wave functions can be readily interpreted in terms of the well known classical VB resonance structures. The total CASVB wave function is identical to the canonical CASSCF wave function. In other words, the MO description and the VB description are equivalent, at least at the level of CASSCF. The CASVB method provides an alternative tool for describing the correlated wave functions.

Similar approaches have been employed by various workers. Lam *et al.*⁵ showed that wave functions in FORS can be expressed in terms of localized configuration-generating MOs which have essentially atomic character. Gordon *et al.*⁶ extended the idea and used it successfully to study the high-valent transition metal complexes. They used the orthogonal spin functions generated by the Kotani–Yamanouchi branching diagrams. Also our method has some relation to the spin-coupled valence bond (SCVB) method of Cooper *et al.*,⁷ where the spin-coupled orbitals and the spin-coupling coefficients are optimized simultaneously. Their LMOs are nonorthogonal while ours are orthogonal. Goddard *et al.*⁸ have proposed the generalized valence bond (GVB) method. GVB has the advantage of compactness, as the wave functions are generally assumed to be formally purely covalent. However, GVB does not offer the clear relationship between the wave function and the various Lewis structure. Hiberty *et al.*⁹ have also developed a general VB method and discussed chemical reactivity and structure.

In Sec. II we will describe in more detail how to transform the canonical CASSCF wave functions to CASVB functions. Applications to benzene, butadiene, and methane will be discussed in Sec. III. A summary will be given in the final section.

II. CASVB METHOD

Let us consider benzene, as an example, with $S=M=0$, where S is the spin quantum number and M specifies the projection of the spin angular momentum along a Z axis. To describe the electronic structure of benzene, we first carried out a standard CASSCF calculation using a basis set of triple zeta quality plus double polarization, ($4s3p2d/2s1p$), taken from Dunning's correlation-consistent basis.¹⁰ A regular hexagonal geometry is used for the ground and excited states with experimental C–C and C–H bond lengths of 1.397 and 1.084 Å,¹¹ respectively. The six valence π orbitals are in the order of energy: $a_{2u}(1b_{1u})$, $e_{1g}(1b_{2g})$, $e_{1g}(1b_{3g})$, $e_{2u}(1b_{1u})$, $e_{2u}(1a_u)$, and $b_{2g}(2b_{3g})$ in D_{6h} symmetry. The symmetry class in D_{2h} group is given in parentheses. They are designated by 3, 2, 1, 1', 2' and 3', respectively. The occupied orbitals in the HF approximation are numbered from the highest one down and the unoccupied orbitals from the lowest one up. The orbitals i and i' are called a conju-

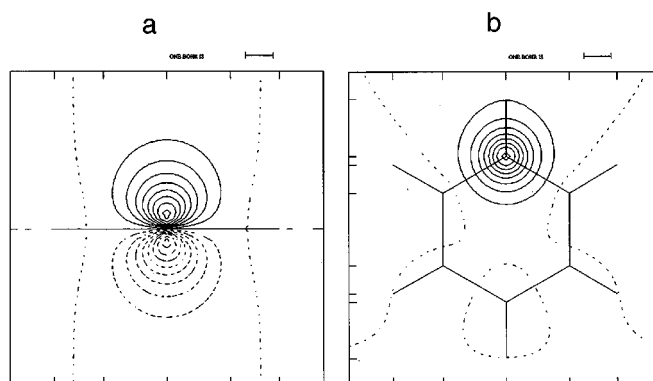


FIG. 1. CAS LMO for benzene. (a) Contours are plotted in a σ_h mirror (perpendicular to the molecular plane). (b) Contours are plotted in the plane 0.3 Å above the σ_h plane.

gated pair and the well-known pairing properties are satisfied. The 1 and 2 are degenerate HOMO and 1' and 2' are degenerate LUMO. The active part of CASSCF formally can be written as

$$\{\pi_3, \pi_2, \pi_1, \pi_{1'}, \pi_{2'}, \pi_{3'}\}^6.$$

The six π electrons are distributed among the six valence π orbitals. We use the abbreviation (n,m) to define the active electrons and active orbitals. Here, n is the number of active electrons and m the number of active orbitals. (n,n) is referred to as a single active space. In the previous study¹² the effect of the enlargement of the active space was studied using the extended active space, where 6 π electrons were distributed among 12 π orbitals. This active space, $(n,2n)$, is referred to as a double active space.

The CASSCF wave function is invariant against unitary transformations among active orbitals. Making use of this orbital arbitrariness, we can construct LMOs. Several approaches for transforming the delocalized MOs into LMOs have been developed.¹³ We used here the Boy's localization procedure¹⁴ to obtain LMOs. In Fig. 1, one of the six π LMOs of benzene is shown. The π LMO nearly always turns out to be well localized on a single atomic center with small localization tails onto the neighboring carbons. Each LMO possesses an identical energy and shape and the LMOs can be transformed into one another by C_6 rotations. Each π LMO resembles the atomiclike $2p$ function although it is deformed symmetrically towards the neighboring carbon atoms on each side. Although very atomic in nature LMOs are still MOs and therefore these LMOs are orthonormal. The localization tails come partly from this orthogonalization constraint. The deviation of the LMOs from the pure atomic $2p$ functions also reflects the mutual polarization of the electronic distribution placed in a molecule.

We now construct the bonded functions with the Rumer spin eigenfunctions based on the LMOs and the full CI is performed within the active space spanned by these bonded functions. That is, the CASSCF function is projected onto the space spanned by the VB functions. All possible configurations with the Rumer spin eigenfunctions are constructed from the active electrons. The phases of the VB structures

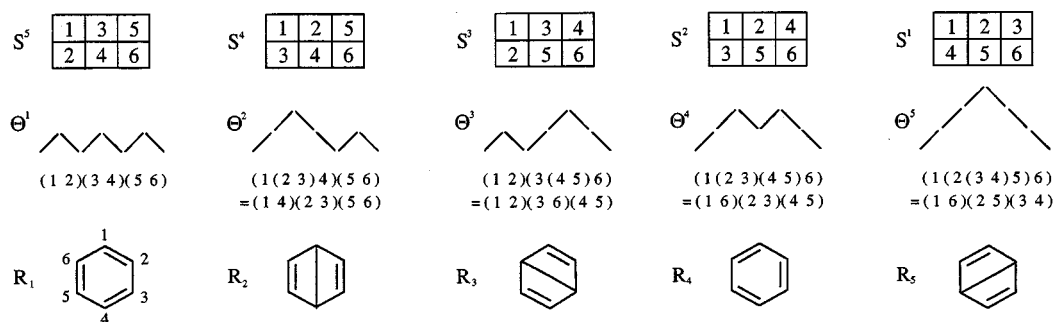


FIG. 2. Standard Young tableaux, branching diagram symbols and the Rumer functions for $N=6$, $S=0$.

are chosen such that all the overlap integrals between any two VB structures are positive. The energy obtained is, of course, identical to that of the canonical CASSCF. This procedure is equivalent to constructing the VB wave function by placing one electron in each π orbital and then combining the spins so as to obtain states of proper spin and Pauli symmetry.

The Rumer spin functions are linearly independent but nonorthogonal to each other. For a system such as benzene of six spins with $S=0$, there are five independent spin couplings. These are specified by the branching diagram or the standard Young tableaux. There is a one-to-one correspondence between spin couplings specified by the standard Young tableaux and the branching diagram symbols and the covalent VB structures. The five standard tableaux (arranged in the last letter sequence) and the spin couplings are given in Fig. 2. The spin coupling in a configuration function based on a particular product is described by a system of parentheses coupling pairs of orbitals in the product. For a given number of electrons N and total spin quantum number S , there will be $N/2 - S$ pairs of orbitals in general, while the $2S$ orbitals remaining unpaired will be associated with dangling left parentheses. Either a left or a right parenthesis is associated with each orbital, and the coupling between them is determined by the usual conventions for associating nested pairs of parentheses in algebraic expressions. A coupled pair of orbitals ($\varphi_i(\dots)\varphi_j$) occupying the i th and j th positions in the orbital product are associated with the spin factor

$$[\alpha(i)\beta(j) - \beta(i)\alpha(j)]/\sqrt{2} \quad \text{if } i \neq j$$

and

$$\alpha(i)\beta(i) \quad \text{if } i = j.$$

The weight of each structure in the VB wave function is sometimes taken as proportional to the square of its coefficient in the wave function. However, because the Rumer spin couplings are not mutually orthogonal, the electron density is not equal to the weighted sum of the density of the various structures. There are several other ways of assigning weights to VB structures. In this paper, we defined the occupation number n_I for the VB structure I as

$$n_I = C_I^* \sum_J S_{IJ} C_J,$$

where the sum goes over all the VB structures. The C_I and S_{IJ} are the coefficient of the VB structure I and the overlap integral between structures I and J , respectively. The n_I add to 1,

$$\sum_I n_I = 1.$$

The n_I give an estimate of the importance of the VB structure.

Our CASVB approach is related to the SCVB theory proposed by Copper *et al.*⁷ In the case of benzene, for example, the spin-coupled wave function composed of five covalent structures is constructed from the nonorthogonal six π orbitals with Rumer spin functions and the spin-coupled orbitals and the spin-coupling coefficients are optimized simultaneously. The orbitals thus obtained are localized on a single atomic center. Then, the spin-coupled wave function is improved through the nonorthogonal CI by adding singly, doubly, and higher order excited configurations (structures) constructed from the spin-coupled orbitals. This is equivalent to introducing the ionic structures to the classical VB wave function composed of covalent structures. When the SCVB wave function includes all possible distributions of the n valence electrons among the n valence orbitals, the result is referred to as full-valence SCVB. This is almost equivalent to the CASVB for n electrons in n orbitals. However, the variational principle tells us that CASVB gives always lower energy than SCVB. Only when the spin-coupled orbitals in a CI expansion are reoptimized simultaneously with the coefficients, the full-valence SCVB becomes identical to the CASVB with a single active space. More extensive nonorthogonal CI can be used to improve the full-valence SCVB by making use of the virtual spin-coupled orbitals. This procedure corresponds to the extension of the active space in the CASSCF method. The principal difficulty with the use of SCVB must be in working with nonorthogonal orbitals. Comparison between CASVB and SCVB results on benzene will be made in the next section.

III. RESULTS AND DISCUSSIONS

A. Benzene

Ab initio VB calculations on benzene reported in the literature have been carried out using no more than minimal

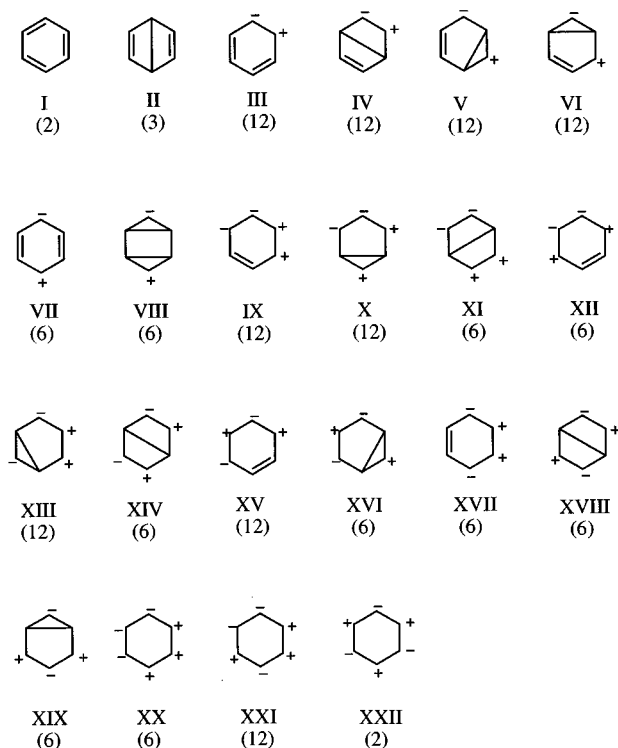


FIG. 3. Rumer diagrams and number of equivalent individual structures for the 1^1A_{1g} symmetry of benzene.

basis sets.^{15,16} Very recently da Silva *et al.*¹⁷ have applied SCVB theory to benzene and studied the electronic structures of its ground and excited states. As discussed previously,¹² benzene is an alternant hydrocarbon and the pairing properties are satisfied even at the CASSCF level. These one-electron symmetry properties were first utilized by Pariser¹⁸ who distinguished the states as so-called “plus” and “minus” ones. Due to the well known relation of the π orbital energy, $\epsilon_i = -\epsilon_{i'} + \text{constant}$, the energy of the configuration obtained by exciting an electron from the π orbital i to the j' is equal to that obtained by excitation from j to i' , even with the inclusion of electronic interaction. The linear combinations of the two degenerate configurations generate the *minus* (−) and *plus* (+) states.

The ground 1^1A_{1g} ($1^1A_{1g}^-$) state is well described by the HF configuration and classified into a *minus* covalent state. In the VB treatment, there are 22 different types of bonding schemes with 175 structures in benzene and these are given in Fig. 3. Each of these bonding schemes gives rise to a linearly independent symmetry function. The number in parentheses in the figure shows the number of equivalent structures in the 1^1A_{1g} symmetry. There are five covalent VB structures, two Kekule (R_1 and R_4) and three Dewar (R_2 , R_3 , and R_5) structures. In Table I we present the structure occupation numbers for the ground state of benzene. For comparison, previous results obtained by Tantardini *et al.*¹⁶ are also listed in the table. The leading VB structures with their structure occupation numbers for the ground and va-

TABLE I. Occupation numbers for $1^1A_{1g}^-$ symmetry structures of benzene.

Symmetry structure	Total occupation numbers, n_i^a	occupation numbers for individual VB	Total occupation numbers, n_i^a (STO basis) ^b
I	0.1565	0.0782	0.222
II	0.0771	0.0257	0.110
III	0.2528	0.0211	0.251
IV	0.1183	0.0099	0.117
V	0.0444	0.0037	0.042
VI	0.0423	0.0035	0.038
VII	0.0247	0.0041	0.023
VIII	0.0079	0.0013	0.007
IX	0.0019	0.0002	0.001
X	0.0046	0.0004	0.003
XI	0.0002	0.0000	0.000
XII	0.0191	0.0032	0.012
XIII	0.0042	0.0004	0.002
XIV	0.0131	0.0022	0.009
XV	0.1157	0.0096	0.086
XVI	0.0230	0.0038	0.016
XVII	0.0178	0.0030	0.011
XVIII	0.0308	0.0051	0.021
XIX	0.0220	0.0037	0.015
XX	0.0000	0.0000	0.000
XXI	0.0072	0.0006	0.003
XXII	0.0162	0.0081	0.010

$$^a n_i = C_i^* \sum_I S_{IJ} C_j$$

^bG. F. Tantardini, M. Raimondi, and M. Simonetta, *J. Am. Chem. Soc.* **99**, 2913 (1977).

lence $\pi \rightarrow \pi^*$ singlet excited states of benzene are shown in Fig. 4.

We arranged the VB structures roughly in three groups according to their character. The first group includes two Kekule covalent structures and the singly and doubly polar structures originated from the Kekule structures. The second group contains the Dewar covalent structures and their singly and doubly polar structures. The ionic structures where an electron is transferred between orbitals centered on nonadjacent atoms are classified into the third group. The grouping is not strict for it is rather difficult to know the origins of doubly and triply polar structures, but the grouping is useful to discuss the character particularly of the excited states.

1. The ground state of benzene

There is an interesting contrast between VB and MO descriptions. In MO theory the aromatic character of benzene is explained in terms of delocalized orbitals. In classical VB theory, benzene is described as a mixture of the two Kekule structures. It is called a resonance hybrid.¹⁹ The ground state of benzene is classified into a covalent state in view of the alternant hydrocarbons. The present CASVB description shows that the most important contributions come from the 2 Kekule, 3 Dewar, and 24 orthopolar (an electron is transferred from one orbital to that centered on an adjacent atom) structures. The occupation number of Dewar structures is about half of that of the Kekule structures. However, the occupation numbers for individual structures in Table I indicate that the Kekule structure is the most important and the next important is the Dewar structure in agreement with that

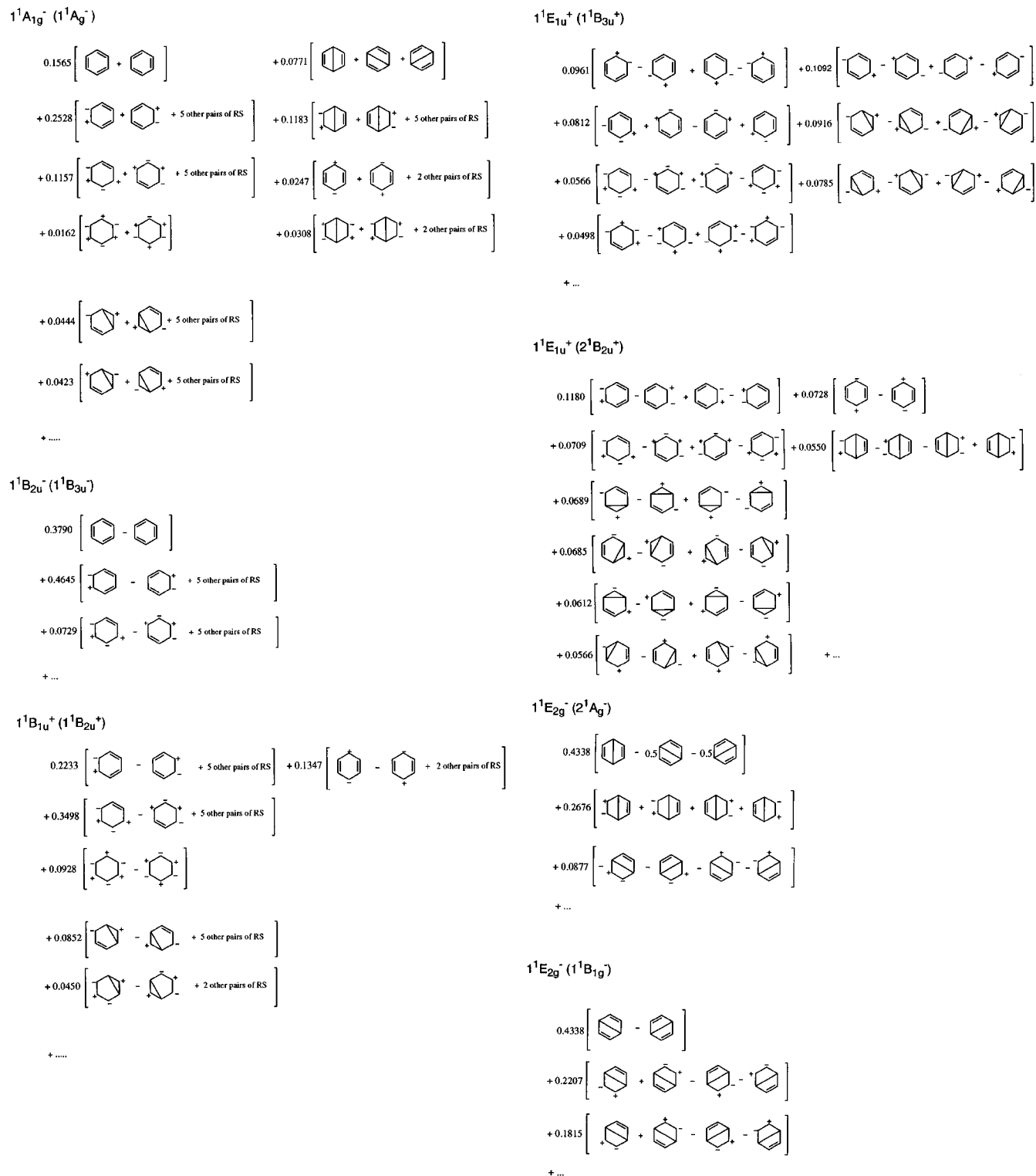


FIG. 4. Description of the ground and excited state CASVB wave functions of benzene. Values are the occupation numbers of the Rumer functions. RS indicates the corresponding symmetry related resonance structures.

commonly expected. It is seen from Table I that the present CASVB has a very similar tendency to the previous VB results calculated with the STO minimum basis set by Tarrantini *et al.*¹⁶

There are two equivalent Kekule structures. The linear

combinations of the two degenerate structures generate the plus and minus states. Their positive combination gives rise to the totally symmetric $1^1A_{1g}^-$ ground state while the negative combination yields the excited $1^1B_{2u}^- (1^1B_{3u}^-)$ as will be discussed later.

TABLE II. CASSCF and MRMP vertical excitation energies (eV) for singlet benzene.^a Comparison with the spin-coupled VB results.^b

Method	Ground state energy (a.u.)	Excitation energy (eV)			
		$1^1B_{2u}^-$	$1^1B_{1u}^+$	$1^1E_{1u}^+$	$1^1E_{2g}^-$
SCVB	-230.788 02	5.43	9.21	10.48	8.83
Full VB					
SCVB	-230.795 21	4.95	7.49	8.43	7.98
Full VB plus CISDT					
CASSCF (6,6)	-230.825 72	4.82	7.91	9.29	8.01
MRMP (6,6)	-231.630 73	4.71	5.83	6.33	7.73
CASSCF (6,12)	-230.844 34	4.89	7.57	8.78	8.04
MRMP (6,12)	-231.629 03	4.67	6.14	6.84	7.71
Exptl.		4.90 ^c	6.20 ^{c,d}	6.94 ^c	7.80 ^e

^aT. Hashimoto, H. Nakano, and K. Hirao, *J. Chem. Phys.* **104**, 6244 (1996).

^bE. C. da Silva, J. Gerratt, D. Cooper, and M. Raimondi, *J. Chem. Phys.* **101**, 3866 (1994).

^cA. Hiraya and K. Shobatake, *J. Chem. Phys.* **94**, 7700 (1991).

^dE. N. Lassetre, A. Skerbele, M. A. Dillon, and K. J. Ross, *J. Chem. Phys.* **48**, 5066 (1968).

^eN. Nakashima, H. Inoue, M. Sumitani, and K. Yoshihara, *J. Chem. Phys.* **73**, 5976 (1980).

One of the aspects of the present method is that this state, though largely covalent, displays a somewhat greater degree of mixing with ionic structures. Note that there is no net charge on any carbon atom. The requirement of ionic structures is due mainly to the fact that the LMOs are orthogonal to each other and not allowed to distort on molecular formation. The ionic structures partially compensate for this. If the orthogonality condition is relaxed and LMOs are reoptimized, the contribution from the ionic structures is expected to be reduced. In fact, Cooper *et al.*⁷ found that the contributions of ionic structures are less significant in their spin-coupled wave function, where the spin-coupled orbitals and the spin-coupling coefficients were optimized simultaneously.

2. Singlet $\pi \rightarrow \pi^*$ excited states of benzene

Now let us discuss the CASVB description of excited states. Table II summarized the excitation energies reported previously.¹² We included results calculated by CASSCF and MRMP with single and double active spaces. For comparison, we only listed SCVB results by da Silva *et al.*¹⁷ There are many MO calculations on the excitation energy of benzene. But the comparison is not the aim of the present paper and they are not cited here.

The excited states of benzene were discussed in detail elsewhere,¹² so only a brief survey of the main features and results follows. The excited states of benzene are classified into the covalent *minus* states and ionic *plus* states with the use of the alternancy symmetry. The covalent *minus* states and ionic *plus* states exhibit different behavior as far as the electron correlation is concerned. In a MO treatment, the electronic excited states can be described in terms of singly, doubly, ..., excited configurations constructed from occupied and unoccupied delocalized orbitals. The ionic *plus* states are

dominated by the single excitations but covalent *minus* states include a large fraction of doubly excited configurations. It is now well known that the dynamic $\sigma-\pi$ polarization effects are significant for the ionic *plus* states since π ionic configurations strongly polarize the σ space. These effects which are almost completely neglected in the CASSCF with π -active orbitals, are taken into account by the second-order perturbation treatment in MRMP. The dynamic $\sigma-\pi$ polarization effects on covalent excited states are usually the same as in the covalent ground state. In general the excitation energies of ionic *plus* states are overestimated considerably at the CASSCF level and the introduction of dynamic $\sigma-\pi$ polarization effects through the second-order perturbation reduces the excitation energies drastically, leading to a good agreement with the experiment. In addition, the enlargement of the active space of the CASSCF functions has proven to represent a great improvement of the description of the ionic states while it has a minor effect on the covalent excited states.

The VB description give a quite different picture for the excitation from the MO description. Excitation process is represented in VB theory in terms of the rearrangement of spin couplings and the charge transfer. The former generates the excited states of covalent nature and the latter gives rise to the ionic excited states. There is a one-to-one correspondence between the covalent VB structure (the covalent perfect pairing structures) and the spin couplings. Thus the rearrangement of spin couplings leads to the shift of the dominant VB structures reciprocally among the covalent VB structures. For example, the Kekule structures ($R_1 + R_4$) are the dominant terms in the ground state of benzene but other covalent VB structures become dominant in the covalent excited states.

In the latter case, an electron transfers from one orbital to that centered on the other atom within a covalent bond. That is, the covalent bond is broken and a new ionic bond is formed. Thus the singly, doubly, ... polar structures are generated from their "parent" covalent (nonpolar), singly, ... polar structures of the ground state, respectively. This implies that there is no mixing with the nonpolar covalent structures in the purely ionic excited states. The structures with highest ionicity are the triply polar ones in benzene. These structures have considerable contributions to the description of the ground state. Table I shows that the triply ionic VB structures of XXII are rather important. However, the completely ionic structures cannot polarize any more in the present level of approximation. This causes a considerable error for the description of the ionic excited states. In the present treatment we distribute six π electrons among six π orbitals and thus obtain six LMOs. More LMOs such as diffuse LMOs, must be prepared to help the polarization if we want to obtain more accurate description. This implies that the active space needs more flexibility. This is the reason why CASSCF with a single active space provides a rather poor description of the ionic excited states.

The dipole transition moment between any two *plus* states or between any two *minus* states is zero in view of the pairing property. That is, only transitions between *plus* and

minus states are allowed (all-*trans*-polyenes and polyacenes have a center of symmetry which gives rise to the selection rules: only $u \rightarrow g$ and $g \rightarrow u$ transitions are allowed). In a VB picture, the dipole transition moment between any two structures with one ionicity difference are nonzero. For example, a covalent structure has the nonzero transition moment only against its singly ionic structures.

The lowest singlet $\pi \rightarrow \pi^*$ excited state was computed to be the ${}^1B_{2u}^-({}^1B_{3u}^-)$. The ${}^1B_{2u}^-$ state is mainly described by HOMO \rightarrow LUMO configurations of $1 \rightarrow 2'$ and $2 \rightarrow 1'$ but also includes a considerable amount of doubly excited configurations in a MO treatment. The present CASSCF gives the excitation energy of 4.82 eV. MRMP predicts it appears at 4.71 eV which shows a good agreement with the experimental value of 4.90 eV.²⁰ The state has a covalent nature and the σ - π polarization effect is almost similar to that in the ground state.

The ${}^1B_{2u}^-$ state is described in a CASVB picture predominantly by a combination of the covalent Kekule and the corresponding orthopolar structures of type III. As mentioned above, two Kekule structures mix with different sign, ($R_1 - R_4$). This is true for the ionic structures. Note that the ratio of occupation numbers between the Kekule structures and the singly ionic structures is similar to that of the ground state. Shaik *et al.*²¹ called the ground and the ${}^1B_{2u}^-$ states of benzene as "twin" states in their Kekule-crossing model to explain the anomalous behavior of the b_{2u} modes in the ${}^1B_{2u}^-$ state. The plus and minus combinations implies that the spin couplings are quite different between these two states. There are no significant contributions from the Dewar structures and the corresponding orthopolar structures (IV).

Second, $\pi \rightarrow \pi^*$ excited states of benzene is the ${}^1B_{1u}^+({}^1B_{2u}^+)$. The state is dominated by singly excited configurations arising from degenerate HOMO \rightarrow LUMO excitations of $1 \rightarrow 1'$ and $2 \rightarrow 2'$ in a MO picture. Thus the state has an ionic nature. The excitation energy calculated by CASSCF with a single active space is 7.91 eV. The introduction of the σ - π polarization effect reduces the excitation energy dramatically. The transition energy computed at the MRMP level is 5.83 eV. However, it underestimates the observed value of 6.20 eV^{20,22} by 0.37 eV. MRMP with a double active space represents a great improvement over that with a single active space. The calculated transition energy of 6.14 eV is very close to the experiment. Accurate description of the ionic states needs flexible active space as mentioned above.

It is seen from Fig. 4 that the state is described by a number of ionic structures. There is no contribution from the covalent structures. The leading ionic structures are the doubly polar structures. These structures come from the orthopolar structures of the ground state. Thus one of the remaining covalent bonds in the VB structures of III is broken and the plus and minus charges are generated so as to favor the electrostatic interactions as much as possible. The next important structures are the orthopolar structures, which originate from the two Kekule structures of the ground state. The parapolar structures must come from the Dewar structures of the ground state. That is, the long bond of the covalent

Dewar structures has been broken and the plus and minus charges are put in para positions. Thus the relative ratios of the occupation numbers of these three leading polar structures are similar to those of the corresponding parent structures in the ground state. The occupation numbers for individual structures indicate that the most important is the triply polar (completely ionic) structures although the total occupation number is not large. The transition to this state is dipole forbidden. This can be identified qualitatively from the fact that the main structures of the ground state are the nonpolar Kekule structures while the ${}^1B_{1u}^+({}^1B_{2u}^+)$ state comprises of the doubly polar structures.

Third, valence excited states are the degenerate ${}^1E_{1u}^+({}^1B_{3u}^+, {}^1B_{2u}^+)$ states. The ${}^1E_{1u}^+({}^1B_{3u}^+)$ state is the *plus* state corresponding to the *minus* ${}^1B_{2u}^-({}^1B_{3u}^-)$ state. The CASSCF wave function of the ${}^1E_{1u}^+({}^1B_{3u}^+)$ is dominated by the singly excited configurations of $1 \rightarrow 2'$ and $2 \rightarrow 1'$, which is different from the *minus* ${}^1B_{2u}^-({}^1B_{3u}^-)$ state. The ${}^1E_{1u}^+({}^1B_{2u}^+)$ state is dominated by the singly excited configurations of $1 \rightarrow 1'$ and $2 \rightarrow 2'$. The states are ionic in nature and the σ - π polarization effect is significant. The MRMP excitation energy with a single active space is computed to be 6.33 eV. The theory underestimates the experimental value of 6.94 eV²² by 0.61 eV. MRMP with a double active space gives the excitation energy of 6.84 eV, which is in good agreement with the experimental 6.94 eV. The transition to ${}^1E_{1u}^+$ is dipole allowed.

The ionic character of the states can easily be found from the CASVB description. Both states are described in terms of many different structures with ionicity. However, we cannot find any predominant VB structures. The most important contributions come from the singly polar structures. This is quite different from the lower ${}^1B_{1u}^+({}^1B_{2u}^+)$ state where the leading structures are the doubly polar structures originated from the ground state orthopolar structures. It is seen that the orthopolar and parapolar structures of the ${}^1E_{1u}^+({}^1B_{3u}^+, {}^1B_{2u}^+)$ states originate from the ground state Kekule and Dewar covalent structures, respectively. We cannot find any contributions from the covalent structures.

The highest valence excited states treated here are the ${}^1E_{2g}^-({}^1A_g^-, {}^1B_{1g}^-)$ of covalent nature. The CASSCF wave function of the ${}^1E_{2g}^-({}^1A_g^-)$ is a mixture of configurations $1 \rightarrow 3'$ and $3 \rightarrow 1'$ but includes a large fraction of the doubly excited configurations $(1)^2 \rightarrow (1')^2$, $1 \rightarrow 2'$, $2 \rightarrow 1'$, ..., etc. The ${}^1E_{2g}^-({}^1B_{1g}^-)$ is also represented by a mixture of configurations $2 \rightarrow 3'$ and $3 \rightarrow 2'$ and the doubly excited configurations. MRMP predicted it lies at 7.73 eV above the ground state, which can be compared to the observed value of 7.80 eV.²³

The states have predominantly a Dewar character with smaller contribution from the corresponding orthopolar VB structures of IV. The ${}^1E_{2g}^-({}^1A_g^-)$ state is represented approximately by $(2R_2 - R_3 - R_5)$ and the ${}^1E_{2g}^-({}^1B_{1g}^-)$ state by $(R_3 - R_5)$. No contribution can be found from the Kekule structures. Thus the Kekule structures give the ground state and the ${}^1B_{2u}^-({}^1B_{3u}^-)$ state and the Dewar structures give the ${}^1E_{2g}^-$ states.

As shown above a VB description gives the picture quite

different from a MO description. The CASVB description has the advantage in affording a clear view of the nature of various states. The covalent states can be described mainly by the covalent VB structures with smaller contributions from the ionic structures. On the other hand, the ionic structures are represented purely by a large number of VB polar structures. There is no mixing with the covalent structures.

Now let us make a comparison between our CASVB results and SCVB results of da Silva *et al.*¹⁷ given in Table II. Although the basis sets used are different, SCVB with full 175 VB structures yields very similar excitation energies to the present CASVB (CASSCF) with a single active space as expected. Also SCVB plus single, double, and triple nonorthogonal CI results are essentially the same as the CASSCF results with an extended active space. It is worth emphasizing that the present CASVB is much easier to calculate and more flexible for improvement than SCVB. da Silva *et al.* concluded in the paper¹⁷ that CASSCF is not necessarily a best prelude to a more extended treatment since it is poor at describing the ionic excited states. We do not agree with this view. The CASSCF wave functions can easily be analyzed in the canonical form and/or in the present CASVB form. CASSCF is not accurate enough from the energetical point of view since it does not include the dynamical correlation. However, the deficiency can be remedied through variational CI or perturbational treatments such as MRMP. We believe that CASSCF is a good prelude to more accurate treatments.

B. Butadiene

Although benzene is the most popular molecule treated in classical VB theory, benzene is a unique molecule due to its high symmetry. Butadiene is a good molecule to examine the usefulness of CASVB. CASSCF functions computed with a single active space (4,4) and the (3s2p1d/2s) basis were transformed into CASVB functions. The experimental geometry was used for *trans*-butadiene.²⁴ As to the excitation energies, we will refer to our previous CASSCF and MRMP results computed at the higher level of theory (MRMP with a double active space and (5s4p3d/3s2p) basis).²⁵ We also calculated *cis*-isomer for comparison. For *cis*-butadiene, we used the geometry optimized at the CASSCF level.

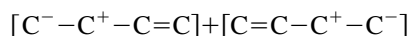
Four π LMOs of *trans*-butadiene are shown in Fig. 5. The π LMOs are well localized again on a single atomic center with small localization tails onto the neighboring carbons. Each π LMO resembles the atomiclike 2p function. However, it has lost the symmetry of the 2p π function due to molecular polarization. A pair of LMO forming a π bond in the ground state repel each other and their lobes lean toward the outside of the π bond. CASVB descriptions for butadiene are shown in Fig. 6. Excitation energies are summarized in Table III. In Fig. 6 the upper value at each VB structure is the occupation number for *trans*-butadiene and the lower one in the parentheses is that for *cis*-isomer. There is no significant difference in CASVB description between *trans*- and *cis*-butadiene except for the $1^1B_u^+$ ($1^1B_2^+$) states.

For butadiene, four singly occupied orbitals lead to two

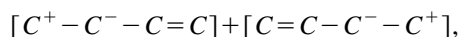
linearly independent VB structures, Kekule-type (R_1) and Dewar-type (R_2) structures. The ground state is mainly comprised of the Kekule-type structure with a smaller contribution from the Dewar-type structure. The simple picture can be written as

$$C_1R_1 + C_2R_2, \quad C_1 \gg C_2.$$

The ground state, though largely covalent, includes contributions from a fairly large number of ionic structures. Considerable contributions come from the two singly ionic structures



and



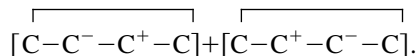
where one electron is transferred in the ethene units.

Note that considerable contributions come from the completely ionic structures. This suggests also that the excited states of ionic nature cannot be described well at the CASSCF level with a single active space.

The $2^1A_g^-$ state is also of covalent nature. In a MO treatment, the state is described by a significant contribution from the singly excited configurations of $1 \rightarrow 2'$ and $2 \rightarrow 1'$ and the doubly excited configuration of $(\text{HOMO})^2 \rightarrow (\text{LUMO})^2$. No definitive experimental data are known on the hidden $2^1A_g^-$ state. MRMP predicted that the transition occurs at 6.31 eV above the ground state. In a VB description the state is expressed predominantly by a Dewar-like structure with a small mixing with the Kekule-type structure

$$C_1R_2 - C_2R_1, \quad C_1 \gg C_2.$$

The spin coupling is different from that in the ground state. The predominant Dewar-type structure suggests that the inversion between single and double bonds will occur upon excitation to this state. This Dewar-type structure comes from the coupling of two simultaneous triplet excitations in ethene units to form an overall singlet spin state. The next important contribution arises from the ionic structures



The central covalent bond of the Dewar-type structure is broken and a new ionic bond is formed. The comparison of the ratio of covalent and ionic structures indicates that the $2^1A_g^-$ state has more covalent character than the $1^1A_g^-$ ground state.

The next excited state is well described by a singly excited $\pi \rightarrow \pi^*$ configuration of HOMO \rightarrow LUMO in a MO description. MRMP placed the energy of the $1^1B_u^+$ state at 6.21 eV above the ground state or 0.3 eV above the experimental intensity maximum of 5.92 eV.^{26,27} Very recently McDiarmid²⁸ placed the pure valence $1^1B_u^+$ state at 6.25 eV, quite close to the MRMP result.

The $1^1B_u^+$ state has an ionic nature which can be readily interpreted in terms of the classical VB resonance structures. The $1^1B_u^+$ state is a mixture of a large number of ionic

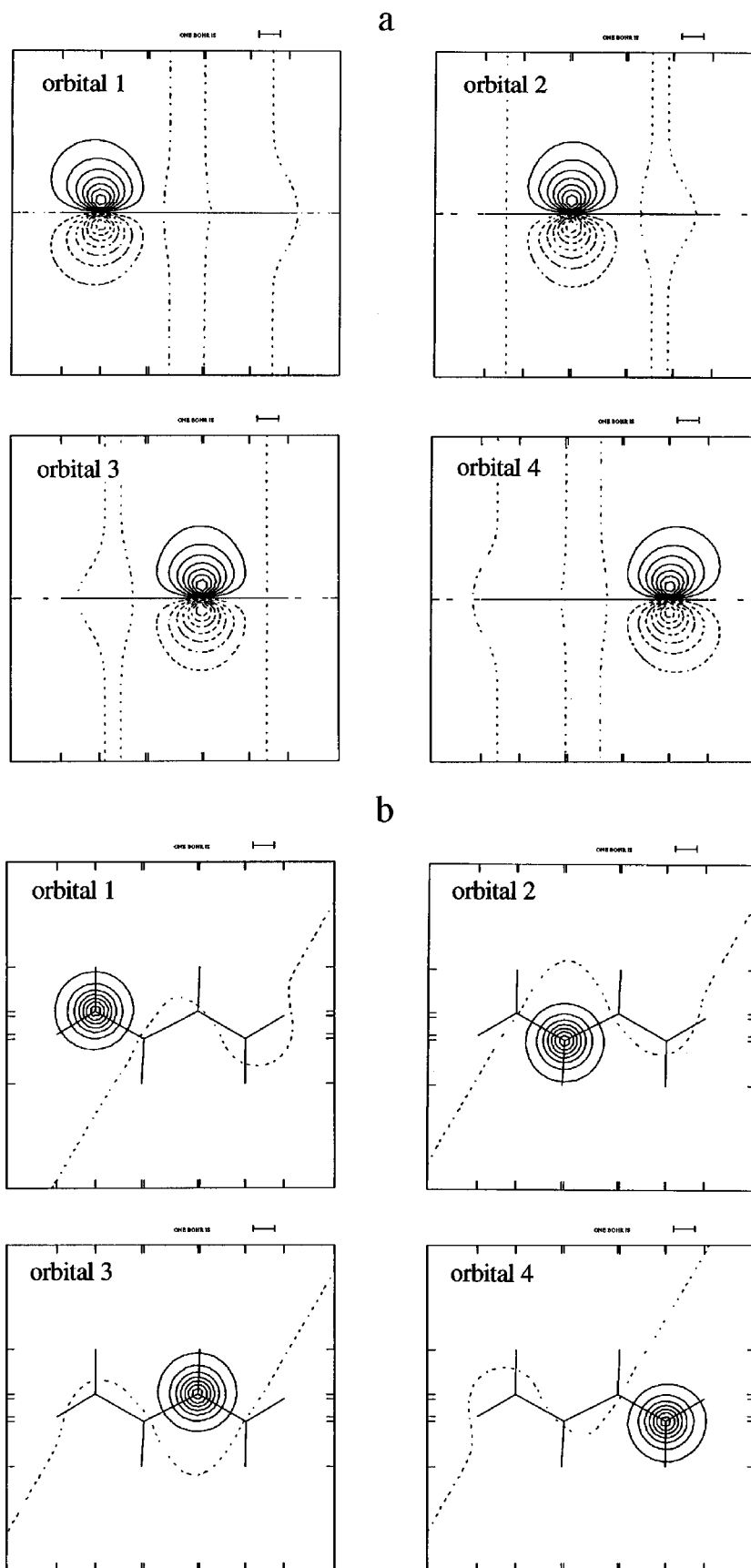
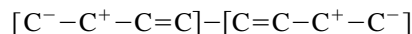


FIG. 5. CAS LMO for *trans*-butadiene. (a) Contours are plotted in a σ_h mirror (perpendicular to the molecular plane). (b) Contours are plotted in the plane 0.3 Å above the σ_h plane.

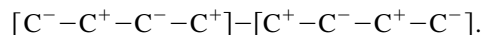
$1^1A_g^-$ (the ground state, covalent)	
0.3960 [C=C-C=C] (0.4134)	+0.0525 [$\overline{C-C-C-C}$] (0.0437)
+0.1970 { [C=C-C=C] + [C=C-C-C*] } (0.1849)	+0.0436 { [$\overline{C-C-C-C}$] + [$\overline{C-C-C-C}$] } (0.0363)
+0.1812 { [C=C-C=C] + [C=C-C-C*] } (0.2022)	+0.0102 { [C=C-C-C*] + [C=C-C-C*] } (0.0067)
+0.0506 { [C=C-C-C*] + [C=C-C-C*] } (0.0540)	+0.0002 { [C=C-C-C*] + [C=C-C-C*] } (0.0000)
+0.0182 [C=C-C-C*] (0.0140)	
+0.0155 [C=C-C-C*] (0.0183)	
+0.0194 { [$\overline{C-C-C-C}$] + [$\overline{C-C-C-C}$] } (0.0142)	
+0.0152 { [$\overline{C-C-C-C}$] + [$\overline{C-C-C-C}$] } (0.0125)	
$2^1A_g^-$ (covalent)	
0.0789 [C=C-C=C] (0.0504)	+0.6059 [$\overline{C-C-C-C}$] (0.6198)
+0.0188 { [C=C-C=C] + [C=C-C-C*] } (0.0248)	+0.2330 { [$\overline{C-C-C-C}$] + [$\overline{C-C-C-C}$] } (0.2469)
+0.0154 { [C=C-C=C] + [C=C-C-C*] } (0.0067)	+0.0040 { [C=C-C-C*] + [C=C-C-C*] } (0.0002)
+0.0038 { [C=C-C-C*] + [C=C-C-C*] } (0.0087)	+0.0002 { [C=C-C-C*] + [C=C-C-C*] } (0.0000)
+0.0037 [C=C-C-C*] (0.0045)	
+0.0028 [C=C-C-C*] (0.0010)	
+0.0218 { [$\overline{C-C-C-C}$] + [$\overline{C-C-C-C}$] } (0.0316)	
+0.0118 { [$\overline{C-C-C-C}$] + [$\overline{C-C-C-C}$] } (0.0055)	
$1^1B_u^+$ (ionic)	
0.1940 { [C=C-C=C] - [C=C-C-C*] } (0.1846)	+0.1900 { [C=C-C=C*] - [C=C-C-C*] } (0.2146)
+0.1488 { [C=C-C-C*] - [C=C-C=C] } (0.1536)	+0.1362 { [C=C-C-C*] - [C=C-C-C*] } (0.1334)
+0.1322 { [$\overline{C-C-C-C}$] - [$\overline{C-C-C-C}$] } (0.1221)	+0.0948 { [$\overline{C-C-C-C}$] - [$\overline{C-C-C-C}$] } (0.0944)
+0.1006 { [$\overline{C-C-C-C}$] - [$\overline{C-C-C-C}$] } (0.0953)	+0.0034 { [C=C-C-C*] - [C=C-C-C*] } (0.0021)

FIG. 6. Description of the ground and excited state CASVB wave functions of *trans*- and *cis*-butadiene. Upper values at the VB structures are occupation numbers or *trans*-butadiene and lower values for *cis*-isomer. The occupation numbers add to 1.

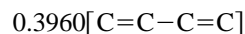
structures. No contribution is found from the covalent structures. The leading terms are the singly and doubly polar structures of



and



Note that singly and doubly ionic structures have nearly the same structure occupation numbers. This can easily be identified if we consider their origins. The former singly ionic structures come from the ground state Kekule-type covalent structure of



and the latter completely ionic structures originate from the following two singly ionic structures of the ground state:

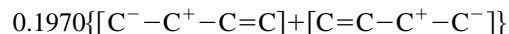


TABLE III. Calculated vertical excitation energies (eV) of *trans*- and *cis*-butadiene singlet states.^a

	CASSCF (4,8) ^a	MRMP (4,8) ^a	Oscillator strength	Expt.
<i>trans</i> -butadiene (C_{2h})				
$2^1A_g^-$	6.67	6.31	Forbidden	
$1^1B_u^+$	7.73	6.21	0.803	5.92, ^b 6.25 ^c
<i>cis</i> -butadiene (C_{2v})				
$2^1A_1^-$	6.56	6.30	0.004	
$1^1B_2^+$	6.88	5.59	0.337	5.5 ^d

^aResults calculated with a double active space and the ($5s4p3d/3s2p$) basis set. The geometry of *cis*-butadiene is optimized by CASSCF with the (4,8) active space and ($4s3p2d/2s$) basis. The optimized terminal C_1-C_2 and central C_2-C_3 bond lengths are 1.472 and 1.337 Å, respectively.

^bO. A. Mosher, W. M. Flicker, and A. Kuppermann, Chem. Phys. Lett. **19**, 332 (1973); J. Chem. Phys. **59**, 6502 (1973); A. Kuppermann, W. M. Flicker, and O. A. Mosher, Chem. Rev. **79**, 77 (1976), Chem. Phys. **30**, 307 (1978); R. McDiarmid, Chem. Phys. Lett. **34**, 130 (1975), J. Chem. Phys. **64**, 514 (1976); K. K. Innes and R. McDiarmid, *ibid.* **68**, 2007 (1978); J. P. Doering and R. McDiarmid, *ibid.* **73**, 3671 (1980), **75**, 2477 (1981).

^cR. McDiarmid, Chem. Phys. Lett. **188**, 423 (1992).

^dM. E. Squillacote, R. S. Sheridan, O. L. Chapman, and F. A. L. Anet, J. Am. Chem. Soc. **101**, 3657 (1979); M. E. Squillacote, T. C. Semple, and P. W. Mui, *ibid.* **107**, 6842 (1985).

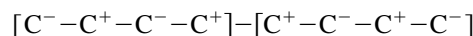
and



The occupation numbers of the respective parent structures are almost the same, which is passed on to their offsprings.

A VB analysis suggests a change in the stability of this state when proceeding from the *trans* to *cis* isomer relative to rotation about the central C-C bond. The first ionic structures shown above have similar stability in the *trans* and *cis* isomers since the electrostatic interactions can be assumed similar. However, the geometry of the *cis* isomer preferentially stabilizes the second type of ionic structures where the distance between the charged ends is greatly reduced. This was pointed out very early in the paper by Cave and Davidson.²⁹

In order to identify this, we also performed MRMP calculations on the *cis* isomer with a double active space and ($5s4p3d/3s2p$) basis set. MRMP yields that *trans*-butadiene is more stable by 2.76 kcal/mol than the *cis* isomer. Note that the leading VB structures of the $1^1B_2^+$ state in *cis*-butadiene turn out to be



with the occupation number of 0.2146. It is seen from Table III that the $1^1B_2^+$ is certainly stabilized relative to the $1^1A_1^-$ state. The transition energies to the covalent $2^1A_g^-$ and $2^1A_1^-$ states in *trans*- and *cis*-butadiene are calculated to be 6.31 and 6.30 eV, respectively. On the other hand, the excitation energy to the $1^1B_2^+$ state in *cis*-butadiene is predicted to be 5.59 eV while the corresponding excitation energy in *trans*-butadiene is 6.27 eV. Thus the *cis* isomer preferentially stabilizes this ionic excited state. This must be a general feature of polyene electronic structure. Polyenes including *cis*-butadiene unit have a lower ionic HOMO-LUMO excited state than the corresponding all-*trans*-polyenes. This point is

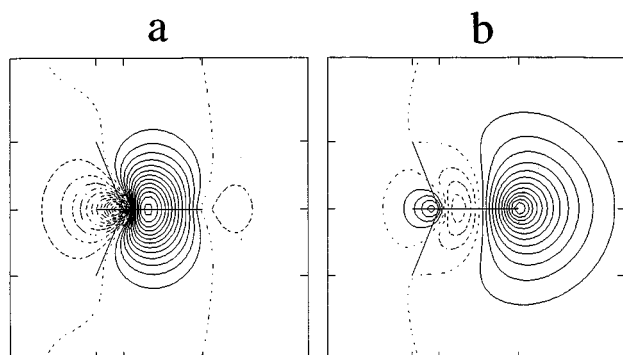


FIG. 7. CAS LMO for methane. (a) Carbon sp^3 . (b) Hydrogen $1s$.

of particular interest because of its relevance to 11-*cis*-retinal which contains *cis*-butadiene unit as a fragment. Further work on retinal will be reported in the future.

C. Methane

Methane is also a molecule to which VB theory was applied in *ab initio* treatment.³⁰ It is thus possible to compare the present CASVB calculations with the previous ones. A tetrahedral geometry with a CH bond length equal to 1.091 Å was used. The basis set used is the double-zeta plus polarization, ($3s2p1d/2s1p$) taken from Dunning's cc-pVDZ.¹⁰ With the restriction that the $1s$ orbital of carbon remains doubly occupied, the eight valence electrons are treated as active electrons and distributed among eight valence orbitals ($2a_1$, $1t_2$, $2t_2$, and $3a_1$) resulting from carbon $2s$ and $2p$ and hydrogen $1s$ orbitals in CASSCF. The energy obtained is $-40.279\,934$ hartree.

Boys' procedure yields four pairs of LMOs. Each pair comprises an orbital predominantly localized on the carbon (\approx carbon sp^3) and a second orbital predominantly localized on the hydrogen (\approx hydrogen $1s$). A pair of these LMOs is shown in Fig. 7. The localization is not complete and it is seen that the localization tails remain on the other atom of the bonding pair. The number of linearly independent symmetry structures belonging to A_1 irreducible representation of the T_d point group is 104. The important VB structures and their occupation numbers are given in Fig. 8. We arranged the VB structures in the order of decreasing occupation numbers for individual structures. Thus, the most important structure is a structure with four covalent bonds. Next are two VB structures with three covalent bonds and one ionic bond. Then follow the structures with two covalent bonds and two ionic bonds. Occupation numbers formed from first four structures yield about 0.6. The leading structures given in Fig. 8 indicate some general features on the importance of each VB structure. The most important factor is the number of CH bonds whether covalent or ionic. For the ionic structures, a structure including highly charged atom becomes unfavorable. A structure with carbon negative is better than carbon positive. These features are consistent with the commonly accepted concepts.

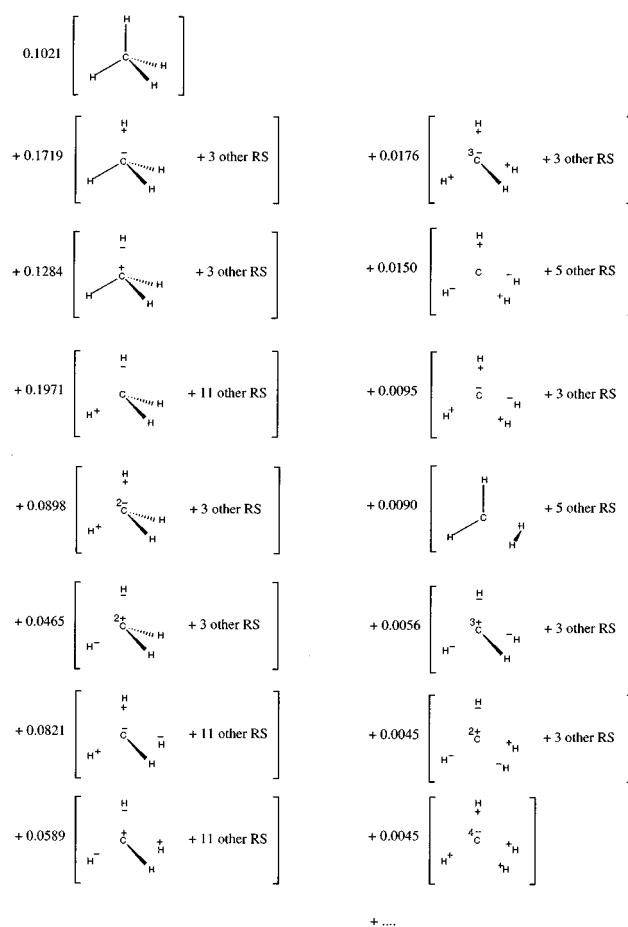


FIG. 8. Description of the CASVB wave function of the ground state methane. RS indicates the corresponding symmetry related resonance structures.

The previous *ab initio* VB calculation on methane was carried out by Raimond *et al.*³⁰ They used a STO minimal set and got an energy of $-40.207\,63$ hartree which is much higher than the present calculation. However, the tendency mentioned above was also observed in their simple VB wave function although they did not give the structure occupation numbers.

The linear combinations of a pair of carbon sp^3 hybrid and hydrogen $1s$ orbitals generate a CH bonding (σ) orbital and its antibonding (σ^*) orbital as shown in Fig. 9. These bonding and antibonding orbitals correspond more closely to the chemist's notion of discrete two-electron bonds. Based on these LMOs, we carried out the full CI calculations within an active space. The wave functions are no longer VB functions. We refer to this approach as the CAS-LMO-CI method. The method is very similar to that proposed by Gordon *et al.*⁶ The only difference is that we are using the Rumer spin functions.

There is an alternative way to define a bonding orbital and its antibonding orbital. When the HF is a good approximation, we can group active orbitals into strongly occupied orbitals and weakly occupied orbitals from their occupation numbers. If the localization is performed separately among strongly occupied orbitals and among weakly occupied orbit-

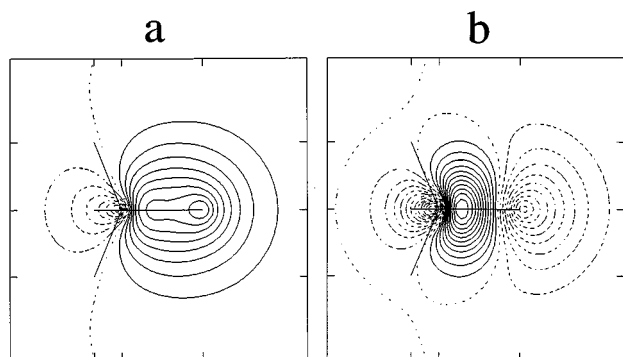


FIG. 9. Bonding and antibonding LMO for methane. (a) CH bonding LMO. (b) CH antibonding LMO.

als, we can obtain bonding and antibonding orbitals, respectively. The CH bond of methane is a nonpolar bond and both definitions yield very similar results but in the case of a polar bond the latter definition may have some advantages.

Table IV lists the first five configurations and their configuration occupation numbers. Configurations are arranged again in order of decreasing occupation number of individual configurations. Occupation numbers formed from first five configurations yield over 0.996. Thus the CAS-LMO-CI approach provides a very compact and clear description of electronic structure of methane. As expected the configuration is predominantly the one with all four CH bonding orbitals doubly occupied. Next are the intrabond doubly excited configurations where two electrons are transferred from one CH bonding orbital to the corresponding antibonding orbital. Then follow the configurations of the interbond single excitation. Thus CAS-LMO-CI also provides an alternative tool to examine the wave function in view of the familiar chemical concept.

IV. SUMMARY

A CASVB approach has been proposed and applied to benzene, butadiene, and methane. Results demonstrate the validity of the CASVB method as a powerful tool for describing the various states of molecules. The main message of this article is that one can obtain a CASVB wave function simply by transforming a canonical CASSCF function with-

TABLE IV. Occupation numbers of CAS-LMO-CI configurations for CH₄.^a

Configurations with a phase factor	Number of equivalent individual configurations	Total occupation numbers
$(1\sigma_1\sigma)(2\sigma_2\sigma)(3\sigma_3\sigma)(4\sigma_4\sigma)$	1	0.9128
$-(1\sigma_1\sigma)(2\sigma_2\sigma)(3\sigma_3\sigma)(4\sigma_4\sigma^*)$	4	0.0264
$(1\sigma_1\sigma)(2\sigma_2\sigma)\{(3\sigma_3\sigma)\{(4\sigma_3\sigma^*) - (4\sigma_4\sigma)(3\sigma_4\sigma^*)\}\}$	12	0.0395
$(1\sigma_1\sigma)(2\sigma_2\sigma)(3\sigma_3\sigma)(4\sigma_4\sigma^*)$	4	0.0082
$-(1\sigma_1\sigma)(2\sigma_2\sigma)(3\sigma_3\sigma^*)(4\sigma_4\sigma^*)$	6	0.0092

^aA coupled pair of orbitals (ij) are associated with the spin factor ($\alpha\beta - \beta\alpha$)/ $\sqrt{2}$ if $i \neq j$, and $\alpha\beta$ if $i = j$. The σ and σ^* indicate CH bonding and antibonding orbitals, respectively.

out any loss of energy. This implies that MO and VB descriptions are equivalent at the CASSCF level of theory. The CASVB provides greater insight than other MO based methods, yet the methods are complimentary, each one providing different perspectives that arise from identical total densities and total energies. Chemists are familiar with LMO and the classical VB resonance concepts which can be found in any organic chemistry textbook. The CASVB forms a useful bridge from molecular orbital theory to the familiar concepts of chemists.

ACKNOWLEDGMENTS

The authors thank Professor Mark S. Gordon (Iowa State University) for valuable discussions. The present research is supported in part by the grant-in-aid for scientific research from the Ministry of Education, Science and Culture of Japan and by the grant from New Energy and Industrial Technology Development Organization (NEDO). One of the authors (K.H.) also thanks the grant by Kawasaki Steel 21st Century Foundation. M.D.'s work was supported in part by the ENvironmental And Molecular Sciences Laboratory Project at the Pacific Northwest National Laboratory (PNNL). PNNL is operated by Battelle Memorial Institute for the U.S. Department of Energy under Contract DE-AC06-76RLO 1830. The computations were carried out on the IBM RS6000-591 workstations. The CASSCF/CASVB wave functions were obtained by a modified version of HONDO96.³¹ The perturbation calculations were performed with the MR2D program.³² Orbital contour maps were plotted using GAMESS program.³³

¹K. Andersson, P. Malmqvist, B. O. Roos, A. J. Sadlej, and K. Wolinski, *J. Phys. Chem.* **94**, 5483 (1990); K. Andersson, P. Malmqvist, and B. O. Roos, *J. Chem. Phys.* **96**, 1218 (1992).

²K. Hirao, *Chem. Phys. Lett.* **190**, 374 (1992); **196**, 397 (1992); **201**, 59 (1993); *Intern. J. Quantum Chem. S* **26**, 517 (1992).

³P. E. Siegbahn, A. Heiberg, B. O. Roos, and B. Levy, *Phys. Scr.* **21**, 323 (1980); B. O. Roos, P. R. Taylor, and P. E. Siegbahn, *Chem. Phys.* **48**, 157 (1980); B. O. Roos, *Intern. J. Quantum Chem. S* **14**, 175 (1980).

⁴K. Ruedenberg, M. W. Schmidt, M. M. Dombek, and S. T. Elbert, *Chem. Phys.* **71**, 41, 51, 65 (1982).

⁵B. Lam, M. W. Schmidt, and K. Ruedenberg, *J. Phys. Chem.* **89**, 2221 (1985).

⁶T. R. Cundari and M. S. Gordon, *J. Am. Chem. Soc.* **113**, 5231 (1991); **114**, 539 (1992).

⁷D. L. Cooper, J. Gerratt, and M. Raimondi, *Nature (London)* **323**, 699 (1986); *Adv. Chem. Phys.* **27**, (Part II) 319 (1987).

⁸W. J. Hunt, P. J. Hay, and W. A. Goddard, *J. Chem. Phys.* **57**, 738 (1972); W. A. Goddard and L. B. Harding, *Annu. Rev. Phys. Chem.* **29**, 363 (1978).

⁹P. C. Hiberty, J. P. Flament, and E. Noizet, *Chem. Phys. Lett.* **189**, 259 (1992); P. Maitre, J. M. Lefour, G. Ohanessian, and P. C. Hiberty, *J. Phys. Chem.* **94**, 4082 (1990).

¹⁰T. H. Dunning, *J. Chem. Phys.* **90**, 1007 (1989).

¹¹A. Langseth and B. P. Stoicheff, *Can. J. Phys.* **34**, 350 (1956).

¹²T. Hashimoto, H. Nakano, and K. Hirao, *J. Chem. Phys.* **104**, 6244 (1996).

¹³C. Edmiston and K. Ruedenberg, *Rev. Mod. Phys.* **53**, 457 (1965).

¹⁴J. M. Foster and S. F. Boys, *Rev. Mod. Phys.* **32**, 300 (1960).

¹⁵J. M. Norbeck and G. Gallup, *J. Am. Chem. Soc.* **96**, 3386 (1974).

¹⁶G. F. Tantardini, M. Raimondi, and M. Simonetta, *J. Am. Chem. Soc.* **99**, 2913 (1977).

¹⁷E. C. da Silva, J. Gerratt, D. L. Cooper, and M. Raimondi, *J. Chem. Phys.* **101**, 3866 (1994).

¹⁸R. Parier, *J. Chem. Phys.* **24**, 250 (1956).

- ¹⁹C. A. Coulson, *Valence*, 2nd ed. (Clarendon, Oxford, 1961), Chap. 9.
- ²⁰A. Hiraya and K. Shobatake, *J. Chem. Phys.* **94**, 7700 (1991).
- ²¹S. Shaik, S. Zilberg, and Y. Haas, *Acc. Chem. Res.* **29**, 211 (1996).
- ²²E. N. Lassetre, A. Skerbele, M. A. Dillon, and K. J. Ross, *J. Chem. Phys.* **48**, 5066 (1968).
- ²³N. Nakashima, H. Inoue, M. Sumitani, and K. Yoshihara, *J. Chem. Phys.* **73**, 5976 (1980).
- ²⁴W. Haugen and M. Traetteberg, *Acta Chem. Scand.* **20**, 1726 (1966).
- ²⁵K. Nakayama, H. Nakano and K. Hirao, *J. Chem. Phys.* (submitted).
- ²⁶A. Kuppermann, W. M. Flicker, and O. A. Mosher, *Chem. Rev.* **79**, 77 (1976); *Chem. Phys.* **30**, 307 (1978).
- ²⁷R. McDiarmid, *Chem. Phys. Lett.* **34**, 130 (1975); *J. Chem. Phys.* **64**, 514 (1976); K. K. Innes and R. McDiarmid, *ibid.* **68**, 2007 (1978).
- ²⁸R. McDiarmid, *Chem. Phys. Lett.* **188**, 423 (1992).
- ²⁹R. J. Cave and E. R. Davidson, *J. Phys. Chem.* **91**, 4481 (1987).
- ³⁰R. Raimondi, W. Campion, and M. Karplus, *Mol. Phys.* **34**, 1483 (1977).
- ³¹M. Dupuis, S. Chin and A. Marquez, in *Relativistic And Electron Correlation Effects in Molecules And Clusters*, edited by G. L. Malli, NATO ASI Series (Plenum, New York, 1992).
- ³²H. Nakano, *J. Chem. Phys.* **99**, 7983 (1993); MR2D Ver.2, H. Nakano, University of Tokyo, 1995.
- ³³M. W. Schmidt, K. K. Baldrige, J. A. Boatz, J. H. Jensen, S. Koseki, M. S. Gordon, K. A. Nguyen, T. L. Windus, and S. T. Elbert, *QCPE Bull.* **10**, 52 (1990).